

# Optimization of Methods for Synthesis and Protonation of Layered Perovskite-Structured Photocatalysts $\text{APb}_2\text{Nb}_3\text{O}_{10}$ (A = Rb, Cs)

S. A. Kurnosenko<sup>a</sup>, A. A. Burov<sup>a</sup>, O. I. Silyukov<sup>a</sup>, V. V. Voytovich<sup>a</sup>, and I. A. Zvereva<sup>a,\*</sup>

<sup>a</sup> *Institute of Chemistry, St. Petersburg State University, St. Petersburg, 199034 Russia*

\**e-mail: irina.zvereva@spbu.ru*

Received November 25, 2022; revised December 9, 2022; accepted December 12, 2022

**Abstract**—Synthesis of layered perovskite-like niobates  $\text{APb}_2\text{Nb}_3\text{O}_{10}$  (A = Rb, Cs), being promising visible light active photocatalysts, has been conducted by the ceramic method under variable conditions to obtain the samples with the highest possible phase purity. The oxides prepared were shown practically not to undergo protonation and hydration of the interlayer space upon keeping in water. Both phases  $\text{APb}_2\text{Nb}_3\text{O}_{10}$  were used to yield corresponding protonated hydrated forms  $\text{H}_x\text{A}_{1-x}\text{Pb}_2\text{Nb}_3\text{O}_{10}\cdot y\text{H}_2\text{O}$  via acid treatment. It was found that the propensity of the samples to the substitution of interlayer cations by protons depends clearly on the  $\text{A}^+$  cation: while the Rb-containing niobate is capable of complete protonation ( $x = 1$ ) upon a single treatment with 6 M nitric acid, the Cs-containing counterpart gives a high enough protonation degree ( $x \geq 0.9$ ) only after several renewals of the acid solution. The protonated niobates obtained were exposed to an additional water treatment under hydrothermal conditions, which allowed producing new hydrated derivatives with the enhanced thermal stability towards interlayer dehydration as compared with the protonated precursors.

**Keywords:** layered perovskite, niobate, protonation, hydration, thermal stability

**DOI:** 10.1134/S1087659622600971

## INTRODUCTION

A number of layered perovskite-like oxides with the general formula  $\text{A}[\text{A}'_{n-1}\text{B}_n\text{O}_{3n+1}]$  (A = Li, Na, K, Rb, Cs; A' = Ca, Sr, Ba, Pb; B = Nb, Ta), belonging to the Dion–Jacobson phases, have been actively investigated since the compounds of the composition  $\text{A}'\text{Ca}_2\text{Nb}_3\text{O}_{10}$  were first obtained [1]. The most well studied among them is the  $\text{KCa}_2\text{Nb}_3\text{O}_{10}$  oxide, whose structure consists of two-dimensional perovskite layers of  $\text{NbO}_6$  octahedra, alternating with  $\text{K}^+$  ions, and  $\text{Ca}^{2+}$  ions occupying 12-coordinated positions in the center of perovskite blocks [2].  $\text{AA}'_2\text{Nb}_3\text{O}_{10}$  oxides can be converted into their protonated forms  $\text{HA}'_2\text{Nb}_3\text{O}_{10}\cdot y\text{H}_2\text{O}$  via the ion exchange in acids [3]. These protonated and hydrated oxides have attracted great attention due to the capability of intercalating amines [4] and exfoliation into nanolayers with the perovskite structure via the intercalation of bulky organic bases [5, 6]. Moreover, the alkaline niobates, their protonated forms as well as exfoliated and restacked composites have been shown to be promising photocatalytic materials [7–9].

Due to the ability to absorb visible light, the special attention has been paid to lead-containing niobates  $\text{APb}_2\text{Nb}_3\text{O}_{10}$  (A = Rb, Cs) [10], which have been actively researched as catalysts for hydrogen production and other photocatalytic processes [11–14].

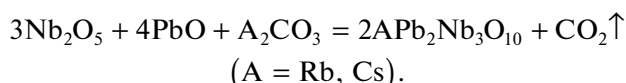
However, it was noted that a number of difficulties arise in the preparation of the alkaline forms of these complex oxides, leading to the formation of nonstoichiometric compounds and impurity phases, including those that can adversely affect the photocatalytic performance as well as the reactivity towards protonation and exfoliation. In view of the above, the present paper focuses on the optimization of the ceramic synthesis method to improve the phase purity of the target niobates  $\text{APb}_2\text{Nb}_3\text{O}_{10}$  (A = Rb, Cs) as well as on their ability to undergo protonation and hydration under various conditions.

## EXPERIMENTAL

Powder X-ray diffraction (XRD) analysis of the samples was conducted on a Rigaku Miniflex II benchtop diffractometer ( $\text{CuK}\alpha$  radiation, angle range  $2\theta = 3^\circ\text{--}60^\circ$ , scanning rate  $10^\circ/\text{min}$ ). Phase composition was determined using Rigaku PDXL2 software. Indexing of the diffraction patterns and calculation of the lattice parameters were performed in the tetragonal system on the basis of all the reflections observed using DiffracPlus Topas software. Elemental composition of the samples was studied by energy-dispersive X-ray spectroscopy (EDX) on a Zeiss Merlin electron microscope equipped with an Oxford Instruments INCAx-act microanalyzer. Raman scattering spectra were recorded on a Horiba LabRam HR800 spec-

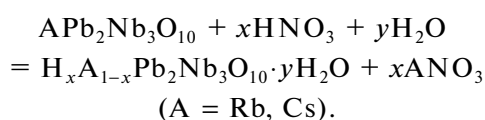
trometer (spectral range 50–4000  $\text{cm}^{-1}$ , He–Ne gas laser 632.8 nm, power 0.6 mW, spectrum accumulation time 60 s, 10 repetitions). Thermogravimetric (TG) analysis was performed on a Netzsch TG 209 F1 Libra thermobalance in a synthetic air atmosphere (temperature range 30–900°C, heating rate 10°C/min). The amounts  $y$  of intercalated water in the protonated and hydrated samples were calculated from the differences between experimental mass losses on TG curves and theoretical ones that would be expected during the complete thermolysis of the samples with the compositions determined by EDX.

$\text{RbPb}_2\text{Nb}_3\text{O}_{10}$  and  $\text{CsPb}_2\text{Nb}_3\text{O}_{10}$  niobates, further abbreviated as  $\text{RPN}_3$  and  $\text{CPN}_3$ , respectively, were synthesized by the conventional high-temperature ceramic method in the air atmosphere using previously dried  $\text{Nb}_2\text{O}_5$  ( $\geq 99.9\%$ , Vekton),  $\text{PbO}$  ( $\geq 99.0\%$ , KhimReaktivSnab) and  $\text{Rb}_2\text{CO}_3$  ( $\geq 99.8\%$ , Sigma-Aldrich) or  $\text{Cs}_2\text{CO}_3$  ( $\geq 99.0\%$ , Sigma-Aldrich) in accordance with the reaction equation:



The oxides were taken in stoichiometric amounts, the carbonates were weighted by default with a 30% excess to compensate for losses during calcination. The reactants were mixed and ground in an agate mortar under a  $n$ -heptane layer at a rate of 0.5 h per 1 g of the batch. The mixture obtained was dried and pelletized into  $\sim 1$  g tablets at a pressure of 50 bar using an Omec PI 88.00 hydraulic press. The tablets were placed into corundum crucibles with lids, calcined in a Nabertherm L-011K2RN muffle furnace and, after cooling down, ground in a mortar. The basic temperature program for  $\text{RPN}_3$  was adopted from the paper [11] and included two-stage calcination at 1000°C for 24 h each one separated by re-grinding of the sample. In the subsequent experiments the synthesis conditions were varied (temperature within 850–1100°C, carbonate excess within 5–50%, one- and two-stage calcination) to improve the phase purity of the product.  $\text{CPN}_3$  was initially prepared according to the literature scheme [15] of one-stage calcination at 1000°C for 24 h, after which the feasibility of the synthesis was also investigated in a wider temperature range (800–1050°C).

To study reactivity of the niobates with regard to protonation and hydration,  $\text{RPN}_3$  and  $\text{CPN}_3$  were exposed to the treatment with aqueous nitric acid of various concentration (2–12 M; 100-fold molar excess) at 25°C under continuous stirring:



The basic treatment duration was 1 day. In the case of 2 M nitric acid, additional 3 and 7 days experiments

with a daily renewal of the acid solution were also conducted. The final samples  $\text{H}_x\text{Rb}_{1-x}\text{Pb}_2\text{Nb}_3\text{O}_{10} \cdot y\text{H}_2\text{O}$  and  $\text{H}_x\text{Cs}_{1-x}\text{Pb}_2\text{Nb}_3\text{O}_{10} \cdot y\text{H}_2\text{O}$  were filtered, rinsed with water to remove the acid residues, dried under ambient pressure and designated as  $\alpha$ -(H,R) $\text{PN}_3$  and  $\alpha$ -(H,C) $\text{PN}_3$ , respectively. Potential partial protonation and hydration were also investigated upon keeping the ceramically synthesized niobates in distilled water without an acid additive for 7 days.

To investigate the possibility of the secondary hydration under hydrothermal conditions giving new protonated hydrated phases, reported earlier for the related niobate  $\text{HCa}_2\text{Nb}_3\text{O}_{10}$  [16], 100 mg of  $\alpha$ -(H,R) $\text{PN}_3$  and  $\alpha$ -(H,C) $\text{PN}_3$  were suspended in 40 mL of distilled water, loaded into 50 mL laboratory high-pressure reactors (autoclaves) and heated for 28 days at various temperatures (100–200°C). After cooling down, the final samples were filtered, dried under ambient pressure and designated as  $\beta$ -(H,R) $\text{PN}_3$  and  $\beta$ -(H,C) $\text{PN}_3$ .

## RESULTS AND DISCUSSION

The products of the high-temperature synthesis were identified by the XRD analysis (Fig. 1). The basic method of  $\text{RPN}_3$  preparation, including two-stage calcination at 1000°C and the use of a 30% carbonate excess, allowed obtaining the target niobate with an insignificant amount of impurity phases (marked with an asterisk). Although the precise determination of these by-phases' composition does not appear possible based on the data available, some assumptions can still be made. The most intense reflections of the impurities are observed at  $2\theta \approx 4.6^\circ$  and  $2\theta \approx 3.8^\circ$ , which corresponds to the interplanar distances of  $\approx 19.4$  and  $\approx 23.0$  Å, respectively. Such reflections may be potentially provided by layered perovskite-structured by-phases with a large  $c$  lattice parameter and, consequently, a greater perovskite layer thickness ( $n = 4$  or 5 niobium-oxygen octahedra) than that of  $\text{RPN}_3$  ( $n = 3$ ). Although the  $n = 4$  and  $n = 5$  phases with the selected elemental composition are not described in the literature, the formation of layered perovskite-like oxides with the perovskite block thickness  $n \geq 3$  is known to be feasible [17].

To improve the phase purity of  $\text{RPN}_3$  samples, the temperature program and carbonate excess were varied. It was found that both re-calcination at 1000°C and increasing synthesis temperature up to 1050 or 1100°C result in rising the intensity of the by-phase reflection at  $2\theta \approx 3.8^\circ$  while the one at  $2\theta \approx 4.6^\circ$  becomes barely visible. Reducing the temperature to 950–900°C gives the product with well pronounced reflections of impurities being comparable in intensity to those of desirable  $\text{RPN}_3$ . When the synthesis temperature is decreased to 850°C, the target niobate ceases to be the main phase in the resulting sample. Rising the carbonate excess up to 50% followed by the

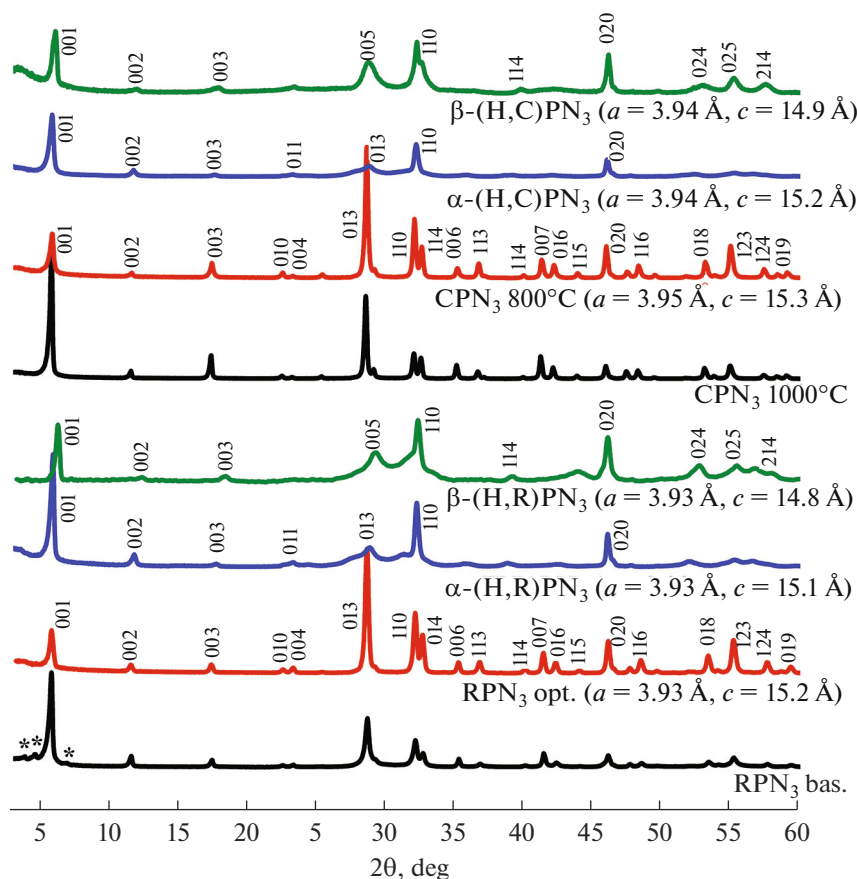


**Fig. 1.** XRD patterns of the niobates prepared according to literature-based (bas.) and optimized (opt.) methods as well as their protonated hydrated forms. An asterisk (\*) denotes impurity phases.

one-stage calcination of the reaction mixture at 1000°C for 24 h gives the target product containing the pronounced impurity phase with the aforementioned  $2\theta \approx 4.6^\circ$  reflection. Re-calcination under the same conditions makes this reflection disappear but the one at  $2\theta \approx 3.8^\circ$  appears instead of it. These results indicate that a heightened carbonate excess promotes the formation of the potentially layered by-phases, one of which ( $2\theta \approx 4.6^\circ$ ) is capable of transforming into another ( $2\theta \approx 3.8^\circ$ ) upon re-calcination and/or temperature rising. In view of the above, it was decided to decrease the carbonate excess to 5% and perform 24 h one-stage calcination at 1000°C. This approach allowed producing RPN<sub>3</sub> in a desired single-phase state and was chosen as an optimal method for the further synthesis of all RPN<sub>3</sub> samples. All the reflections on the XRD pattern of the product (Fig. 1) were successfully indexed in the tetragonal system and the lattice parameters calculated were found to be in good consistency with the literature data [18]. Despite the fact that RPN<sub>3</sub> is well known in the literature [10–13, 18, 19], the aforementioned optimized method for its preparation appears to be a novel and practically significant result since many of the available publications

do not allow evaluating RPN<sub>3</sub>'s phase purity (XRD profiles are shown without the low-angle region, are not presented at all or demonstrate clearly the presence of by-phases).

In the case of CPN<sub>3</sub>, the basic preparation method (one-stage calcination at 1000°C for 24 h with a 30% carbonate excess) resulted in the formation of the target niobate not containing noticeable crystalline impurities (Fig. 1). The same product was also successfully obtained at 1050°C. However, the final tablets of both samples taken after calcination were found to be deformed like a concave lens, which points to the potential melting out of components from the tablets at high temperatures. Moreover, a further EDX analysis showed the products to have lower lead content than in the expected niobate formula. In view of this, the synthesis temperature was decreased to 850°C and then to 800°C to reduce the probability of lead oxide melting out from the reaction zone. The final samples turned out to be single-phase and the tablets were not deformed, although the Nb : Pb ratio = 3 : 1.85 (Table 1) still was somewhat different from the theoretically expected 3 : 2. The XRD pattern of CPN<sub>3</sub> was success-

**Table 1.** Quantitative compositions of the niobates in the form  $H_xA_{1-x}Pb_2Nb_3O_{10} \cdot yH_2O$  (protonation degree  $x$ , amount of intercalated water  $y$ , measured Nb : Pb ratio)

Sample, preparation details	$x$	$y$	Nb : Pb
RPN <sub>3</sub>	—	—	3 : 1.95
RPN <sub>3</sub> water-treated	0.05	—	—
$\alpha$ -(H,R)PN <sub>3</sub>	12 M HNO <sub>3</sub> , 1 day	0.74	3 : 1.60
	6 M HNO <sub>3</sub> , 1 day	0.98	3 : 1.65
$\beta$ -(H,R)PN <sub>3</sub>	1.00	1.00	—
CPN <sub>3</sub>	—	—	3 : 1.85
CPN <sub>3</sub> water-treated	0.00	—	—
$\alpha$ -(H,C)PN <sub>3</sub>	6 M HNO <sub>3</sub> , 1 day	0.92	3 : 1.80
	6 M HNO <sub>3</sub> , 3 days, daily renewal	0.85	3 : 1.45
	2 M HNO <sub>3</sub> , 3 days, daily renewal	0.80	3 : 1.55
	2 M HNO <sub>3</sub> , 7 days, daily renewal	0.95	3 : 1.50
$\beta$ -(H,C)PN <sub>3</sub>	0.95	0.97	—

fully indexed in the tetragonal system with a slightly smaller  $c$  lattice parameter as compared to that of RPN<sub>3</sub> (Fig. 1) due to the difference in the radii of the interlayer alkali cations.

The water treatment of RPN<sub>3</sub> and CPN<sub>3</sub> for 7 days did not lead to any perceptible changes on the XRD patterns and TG curves of the samples (not shown) that could point to the potential water intercalation into the interlayer space. According to the EDX data (Table 1), the resulting protonation degree in the structure of RPN<sub>3</sub> did not exceed  $x = 0.05$  and, in the case of CPN<sub>3</sub>, there was no evidence of protonation at all. Such behavior of the samples in question is generally typical of related niobates  $AA'_2Nb_3O_{10}$  ( $A = K, Rb, Cs$ ;  $A' = Ca, Sr$ ), whose quantitative protonation and hydration upon the contact with water are not known in the literature.

The interlayer cations of RPN<sub>3</sub> and CPN<sub>3</sub> may be substituted by protons in aqueous solutions of acids. In particular, a 1 day treatment of RPN<sub>3</sub> with an excess of either 6 M or 12 M nitric acid allows obtaining a completely protonated form of the niobate denoted as  $\alpha$ -(H,R)PN<sub>3</sub> ( $x = 1.00$ , Table 1). However, since the samples treated with 12 M nitric acid gave strongly broadened XRD reflections (not shown), the further experiments were carried out using a 6 M or more diluted acid. At the same time, complete protonation of CPN<sub>3</sub> proved to be a more challengeable problem: the similar 1 day treatment with 6 M nitric acid resulted in only a half substitution degree ( $x = 0.50$ , Table 1). To heighten the latter, the experiment durations were increased up to 3 and 7 days and the acid solution was renewed daily. The sample obtained via the 7 days treatment with 2 M nitric acid underwent practically complete interlayer protonation ( $x = 0.95$ ,

Table 1), was denoted as  $\alpha$ -(H,C)PN<sub>3</sub> and used in further studies.

Both protonated niobates represent single-phase samples and have a slightly contracted interlayer space as compared with that of the initial compounds (lower  $c$  parameter, Fig. 1) due to the substitution of bulky alkali cations with protons and water molecules. However, the XRD patterns of  $\alpha$ -(H,R)PN<sub>3</sub> and  $\alpha$ -(H,C)PN<sub>3</sub> are not completely identical because of different protonation conditions and potential influence of residual cesium cations. The EDX analysis of the protonated niobates revealed the lowering of lead content in the samples upon acid treatments. For instance,  $\alpha$ -(H,C)PN<sub>3</sub> exhibits a Nb : Pb ratio 3 : 1.50 instead of expected 3 : 2 and the lead loss rises with increasing acid concentration and the reaction duration (Table 1). The fact observed may be caused by both acid washout of lead from the perovskite lattice and dissolution of amorphous lead oxide, potentially presented in the samples. The both cases should probably point to the presence of defects in the niobate structure associated with the lead vacancies.

Protonation and hydration of the niobates is accompanied by characteristic changes seen in their Raman scattering spectra (Fig. 2). Particularly, the band of a symmetric stretching mode of axial Nb—O bonds ( $931\text{ cm}^{-1}$ ) splits into some new bands, apparently, due to non-equivalent surroundings of the interlayer oxygen anions (associated with proton, associated with hydroxonium, bare oxygen). Having said so, the most intense of axial Nb—O vibrational bands corresponds to  $961\text{ cm}^{-1}$ . This frequency increase originates from the substitution of a relatively heavy alkali cation associated with the oxygen ionically (Nb—O<sup>-</sup>A<sup>+</sup>,  $A = Rb$  or  $Cs$ ) by a lightweight proton bound more covalently (Nb—O—H). In addition, the spectra

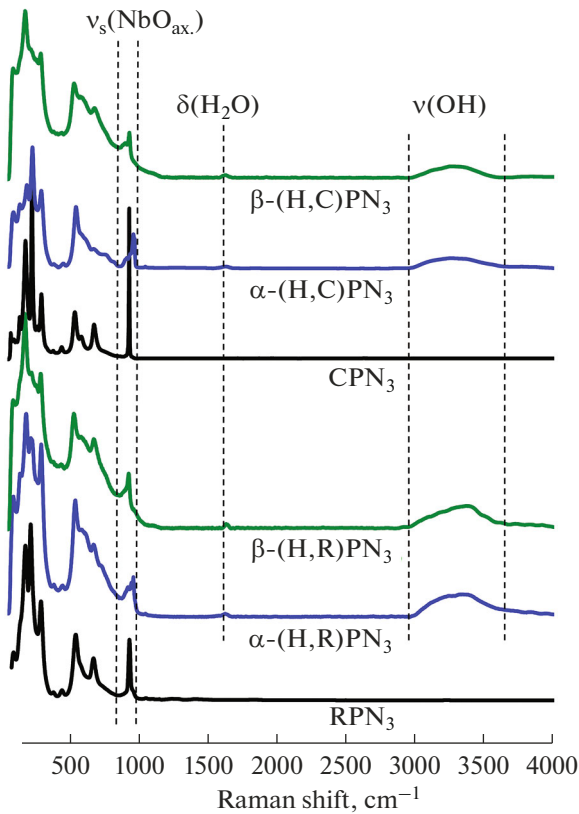


**Fig. 2.** Raman scattering spectra of the initial niobates and their protonated hydrated forms. The range of 1500–4000  $\text{cm}^{-1}$  is upscaled by 15 times.

of the protonated samples exhibit stretching bands of hydroxy groups (3000–3600  $\text{cm}^{-1}$ ) and bending of intercalated water molecules (1625–1630  $\text{cm}^{-1}$ ).

The mass loss during thermolysis of the protonated samples (Fig. 3) is observed predominantly at temperatures up to 400°C and corresponds to two main processes – deintercalation of the interlayer water and decomposition of the protonated niobate itself. However, unlike the case of related niobates  $\text{HA}'_2\text{Nb}_3\text{O}_{10}$  ( $A' = \text{Ca}, \text{Sr}$ ) [20, 21], the mass loss sections are strongly overlapping, which makes it practically impossible to separate them and calculate a protonation degree  $x$  and intercalated water amount  $y$  directly from the TG data [22]. In this connection, the  $y$  values for the protonated hydrated samples were calculated from the differences between experimental mass losses on TG curves and theoretical ones that would be expected during the complete thermolysis of the samples having the compositions determined by EDX. As a result, it was established that the products of protonation contain 0.7–1.0 water molecules per niobate formula unit and this amount depends on the conditions of the acid treatment (Table 1).

To investigate the possibility of the secondary hydration under hydrothermal conditions, reported earlier for the related niobate  $\text{HCa}_2\text{Nb}_3\text{O}_{10}$  [16],  $\alpha$ -(H,R)PN<sub>3</sub> and  $\alpha$ -(H,C)PN<sub>3</sub> were exposed to the water treatment in high-pressure reactors at various temperature for 28 days. The samples obtained at 100°C were revealed to be structurally identical to the

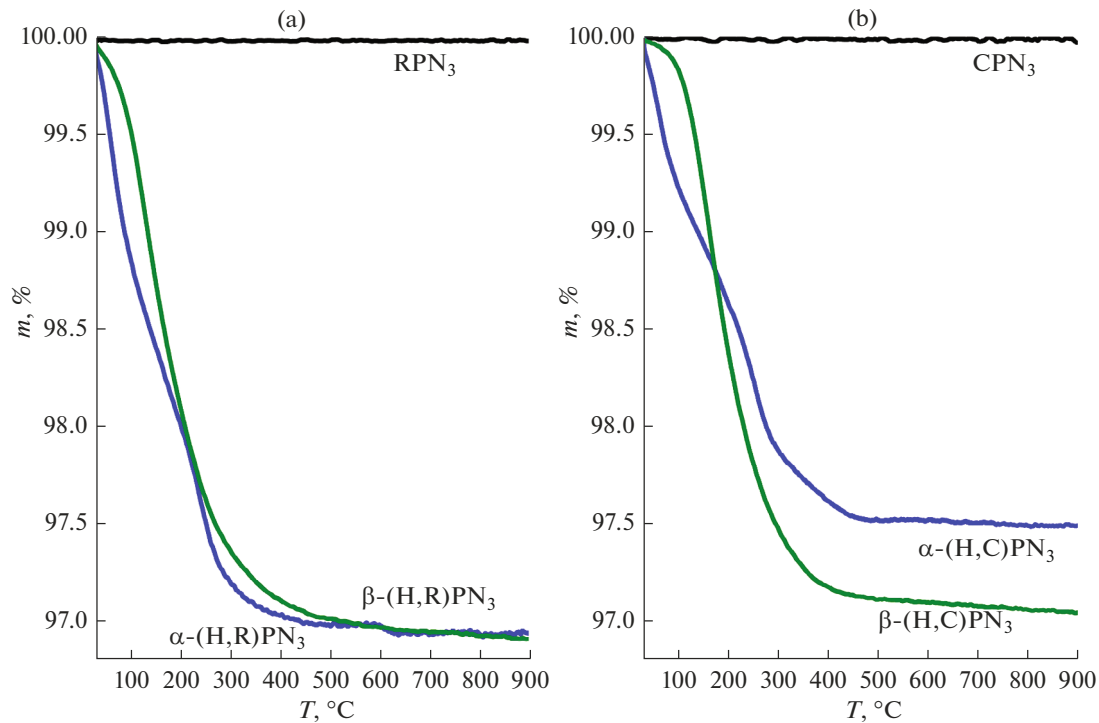


**Fig. 3.** TG curves of the initial niobates and their protonated hydrated forms.

precursors taken. However, when the temperature was 150°C, the protonated niobates experienced the interlayer space contraction by 0.3 Å and were further considered as new phases denoted as  $\beta$ -(H,R)PN<sub>3</sub> and  $\beta$ -(H,C)PN<sub>3</sub> (Fig. 1). The hydrothermal water treatment at 200°C led to the partial decomposition of the protonated phases.

Unlike HCa<sub>2</sub>Nb<sub>3</sub>O<sub>10</sub> [16], the niobates under study do not experience such pronounced structural transformations, observed from the XRD patterns, upon the hydrothermal treatment. Despite the narrowed interlayer space,  $\beta$ -(H,R)PN<sub>3</sub> and  $\beta$ -(H,C)PN<sub>3</sub> proved to be slightly more hydrated compounds than the precursors used (Table 1). Moreover, the  $\beta$ -forms of the niobates are distinguished from the  $\alpha$ -ones by a low-frequency shift of the symmetric stretching mode of axial Nb–O bonds from 961 to 925–930 cm<sup>-1</sup> in the Raman spectra (Fig. 2), which may point to significantly stronger bonding between the interlayer oxygens and water molecules. According to the TG analysis data (Fig. 3), the  $\beta$ -forms demonstrate greater thermal stability towards water deintercalation: while the  $\alpha$ -forms start to liberate interlayer water even at 30–40°C, the  $\beta$ -ones achieve a high rate of dehydration only after 100°C. All these facts together indicate that the products of hydrothermal treatment are characterized by a denser and stronger fixation of water molecules in the interlayer space, which increases the stability towards the interlayer dehydration.

## CONCLUSION

In this research, the high-temperature solid-phase synthesis of layered perovskite-structured niobates APb<sub>2</sub>Nb<sub>3</sub>O<sub>10</sub> (A = Rb, Cs) was carried out under various conditions to achieve the highest possible phase purity of the products. It was shown that the Rb-containing niobate can be prepared in a single-phase state via the one-stage calcination of the reaction mixture, containing a 5% rubidium excess, at 1000°C for 24 h. The synthesis of the Cs-containing niobate was found feasible in a wide temperature range (800–1050°C), although lower temperatures are preferable to reduce the probability of melting out of lead oxide. The niobates prepared were shown to be practically incapable of interlayer protonation upon keeping in water. Their protonated hydrated forms were prepared via acid treatment. It was found that, ceteris paribus, the propensity of the samples to the substitution of interlayer cations by protons depends clearly on the specific A<sup>+</sup> cation: while the Rb-containing niobate is capable of complete protonation ( $x = 1$ ) upon a single treatment with 6 M nitric acid, the Cs-containing counterpart gives a high enough protonation degree ( $x \geq 0.9$ ) only after several renewals of the acid solution. The protonated niobates obtained were exposed to an additional water treatment under hydrothermal conditions, which allowed producing new hydrated derivatives

with the enhanced thermal stability towards interlayer dehydration as compared with the protonated precursors. The data obtained are of high importance in view of the potential use of the niobates in question as visible light active photocatalysts for hydrogen generation, environmental remediation and other purposes.

## ACKNOWLEDGMENTS

Authors are grateful to the St. Petersburg State University Research Park: Centre for X-ray Diffraction Studies, Interdisciplinary Centre for Nanotechnology, Centre for Thermal Analysis and Calorimetry, Centre for Optical and Laser Research.

## FUNDING

The research was supported by the Russian Science Foundation (grant no. 19-13-00184).

## CONFLICT OF INTEREST

The authors declare that the research was conducted in the absence of any commercial or financial relationships that could be construed as a potential conflict of interest.

## REFERENCES

1. Dion, M., Ganne, M., and Tournoux, M., Nouvelles familles de phases MIMII<sub>2</sub>Nb<sub>3</sub>O<sub>10</sub> a feuillets ‘perovskites,’ *Mater. Res. Bull.*, 1981, vol. 16, no. 11, pp. 1429–1435.
2. Fukuoka, H., Isami, T., and Yamanaka, S., Crystal structure of a layered perovskite niobate KCa<sub>2</sub>Nb<sub>3</sub>O<sub>10</sub>, *J. Solid State Chem.*, 2000, vol. 151, no. 1, pp. 40–45.
3. Jacobson, A.J., Lewandowski, J.T., and Johnson, J.W., Ion exchange of the layered perovskite KCa<sub>2</sub>Nb<sub>3</sub>O<sub>10</sub> by protons, *J. Less Common Met.*, 1986, vol. 116, no. 1, pp. 137–146.
4. Jacobson, A.J., Johnson, J.W., and Lewandowski, J., Intercalation of the layered solid acid HCa<sub>2</sub>Nb<sub>3</sub>O<sub>10</sub> by organic amines, *Mater. Res. Bull.*, 1987, vol. 22, no. 1, pp. 45–51.
5. Jacobson, A.J., Johnson, J.W., and Lewandowski, J.T., Interlayer chemistry between thick transition-metal oxide layers: Synthesis and intercalation reactions of K[Ca<sub>2</sub>Na<sub>n-3</sub>Nb<sub>n</sub>O<sub>3+1</sub>] ( $3 \leq n \leq 7$ ), *Inorg. Chem.*, 1985, vol. 24, no. 23, pp. 3727–3729.
6. Schaak, R.E. and Mallouk, T.E., Prying apart Ruddlesden–Popper phases: Exfoliation into sheets and nanotubes for assembly of perovskite thin films, *Solid State Ionics*, 2000, vol. 12, no. 11, pp. 3427–3434.
7. Domen, K., Yoshimura, J., Sekine, T., Kondo, J., Tanaka, A., Maruya, K., and Onishi, I., A novel series of photocatalysts with an ion-exchangeable layered structure of niobate, *Catal. Lett.*, 1990, vol. 4, pp. 339–343.
8. Oshima, T., Ishitani, O., and Maeda, K., Non-sacrificial water photo-oxidation activity of lamellar calcium niobate induced by exfoliation, *Adv. Mater. Interfaces*, 2014, vol. 1, no. 7, pp. 2–5.

9. Sabio, E.M., Chamousis, R.L., Browning, N.D., and Osterloh, F.E., Photocatalytic water splitting with suspended calcium niobium oxides: Why nanoscale is better than bulk—A kinetic analysis, *J. Phys. Chem. C*, 2012, vol. 116, no. 4, pp. 3161–3170.
10. Subramanian, M.A., Gopalakrishnan, J., and Sleight, A.W., New layered perovskites:  $\text{ABiNb}_2\text{O}_7$  and  $\text{APb}_2\text{Nb}_3\text{O}_{10}$  ( $A = \text{Rb}$  or  $\text{Cs}$ ), *Mater. Res. Bull.*, 1988, vol. 23, no. 6, pp. 837–842.
11. Yoshimura, J., Ebina, Y., Kondo, J., Domen, K., and Tanaka, A., Visible light induced photocatalytic behavior of a layered perovskite type niobate,  $\text{RbPb}_2\text{Nb}_3\text{O}_{10}$ , *J. Phys. Chem.*, 1993, vol. 97, no. 9, pp. 1970–1973.
12. Hu, Y., Shi, J., and Guo, L., Enhanced photocatalytic hydrogen production activity of chromium doped lead niobate under visible-light irradiation, *Appl. Catal. A*, 2013, vol. 468, pp. 403–409.
13. Zheng, B. Mao, L., Shi, J., Chen, Q., Hu, Y., Zhang, G., Yao, J., and Lu, Y., Facile layer-by-layer self-assembly of 2D perovskite niobate and layered double hydroxide nanosheets for enhanced photocatalytic oxygen generation, *Int. J. Hydrogen Energy*, 2021, vol. 46, no. 69, pp. 34276–34286.
14. Hu, Y. and Guo, L., Rapid preparation of perovskite lead niobate nanosheets by ultrasonic-assisted exfoliation for enhanced visible-light-driven photocatalytic hydrogen production, *ChemCatChem.*, 2015, vol. 7, no. 110, pp. 584–587.
15. Fang, M., Kim, C.H., and Mallouk, T.E., Dielectric properties of the lamellar niobates and titanoniobates  $\text{AM}_2\text{Nb}_3\text{O}_{10}$  and  $\text{ATiNbO}_5$  ( $A = \text{H}, \text{K}, \text{M} = \text{Ca}, \text{Pb}$ ), and their condensation products  $\text{Ca}_4\text{Nb}_6\text{O}_{19}$  and  $\text{Ti}_2\text{Nb}_2\text{O}_9$ , *Chem. Mater.*, 1999, vol. 11, pp. 1519–1525.
16. Shelyapina, M.G. Silyukov, O.I., Andronova, E.A., Nefedov, D.Y., Antonenko, A.O., Missyul, A., Kurnosenko, S.A., and Zvereva, I.A.,  $^1\text{H}$  NMR study of the  $\text{HCa}_2\text{Nb}_3\text{O}_{10}$  photocatalyst with different hydration levels, *Molecules*, 2021, vol. 26, no. 19, p. 5943.
17. Rodionov, I.A. and Zvereva, I.A., Photocatalytic activity of layered perovskite-like oxides in practically valuable chemical reactions, *Russ. Chem. Rev.*, 2016, vol. 85, no. 3, pp. 248–279.
18. Ziegler, C. Dennenwaldt, T., Weber, D., Duppel, V., Kamella, C., Podjarski, F., Tuffy, B., Moudrakovski, I., Scheu, C., and Lotsch, B.V., Functional engineering of perovskite nanosheets: Impact of lead substitution on exfoliation in the solid solution  $\text{RbCa}_{2-x}\text{Pb}_x\text{Nb}_3\text{O}_{10}$ , *Z. Anorg. Allgem. Chem.*, 2017, vol. 643, no. 21, pp. 1668–1680.
19. Liou, Y. and Wang, C.M., Energetic characterizations of particulate  $\text{RbPb}_2\text{Nb}_3\text{O}_{10}$  electrodes, *J. Electrochem. Soc.*, 1996, vol. 143, no. 5, pp. 1492–1498.
20. Yafarova, L. V. Silyukov, O.I., Myshkovskaya, T.D., Minich, I.A., and Zvereva, I.A., New data on protonation and hydration of perovskite-type layered oxide  $\text{KCa}_2\text{Nb}_3\text{O}_{10}$ , *J. Therm. Anal. Calorim.*, 2021, vol. 143, no. 1, pp. 87–93.
21. Hong, Y. and Kim, S.-J., Intercalation of primary diamines in the layered perovskite oxides,  $\text{HSr}_2\text{Nb}_3\text{O}_{10}$ , *Bull. Korean Chem. Soc.*, 1996, vol. 17, no. 8, pp. 730–735.
22. Zvereva, I.A., Silyukov, O.I., and Chislov, M.V., Ion-exchange reactions in the structure of perovskite-like layered oxides: I. Protonation of  $\text{NaNdTiO}_4$  complex oxide, *Russ. J. Gen. Chem.*, 2011, vol. 81, no. 7, pp. 1434–1441.